Supplementary Information (SI) for Nanoscale.

A Narrow-Bandgap Conjugated-Polymer/MoS_2 Hybrid Photodetector for Room Temperature Shortwave Infrared Detection up to 2000 nm

Misbah Younas[a,b], Juanxia Wu[a*], Weirong Li[c], Xingxin Shao[c], Zunaira Urooj[a,b], Muhammad Ahsan Iqbal[d], Muhammad Asif[a,b], Tariq Abbas[a,b], Jun Liu[c*], Liming Xie[a,b*]

[a]*CAS Key Laboratory of Standardization and Measurement for Nanotechnology, National Center for Nanoscience and Technology, Beijing 100190, P. R. China*

[b]*University of Chinese Academy of Sciences, Beijing 100049, P. R. China*

[c]*State Key Laboratory of Polymer Science and Technology, Changchun Institute of Applied Chemistry Chinese Academy of Sciences, Changchun 130022, P. R. China*

[d]*Guangdong Provincial Key Laboratory of Intelligent Disaster Prevention and Emergency Technologies for Urban Lifeline Engineering, School of Environment and Civil Engineering, Dongguan University of Technology, Dongguan, 523808, P. R. China*

To whom correspondence should be addressed: wujuanxia@nanoctr.cn, liujun@ciac.ac.cn

xielm@nanoctr.cn

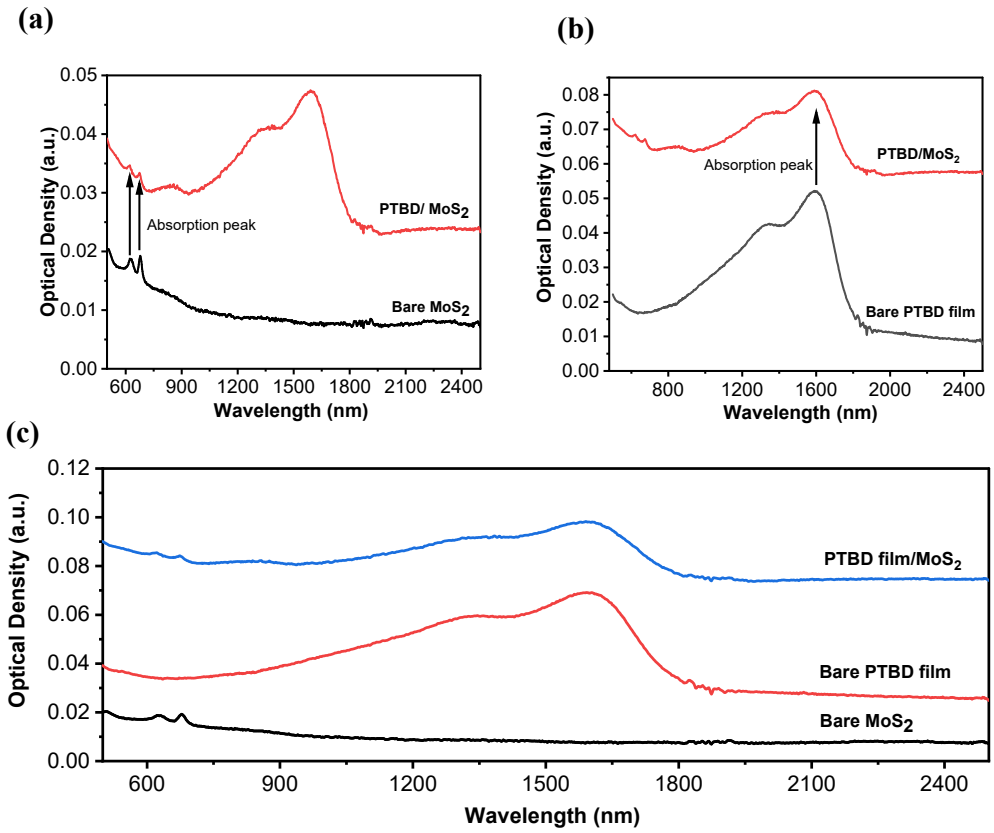

Figure S1. Optical absorption spectra of (a) Bare PTBD and PTBD/MoS_2, b) Bare MoS_2 and PTBD/MoS_2, (c) Combined spectra of bare MoS_2, bare PTBD and PTBD/MoS_2.

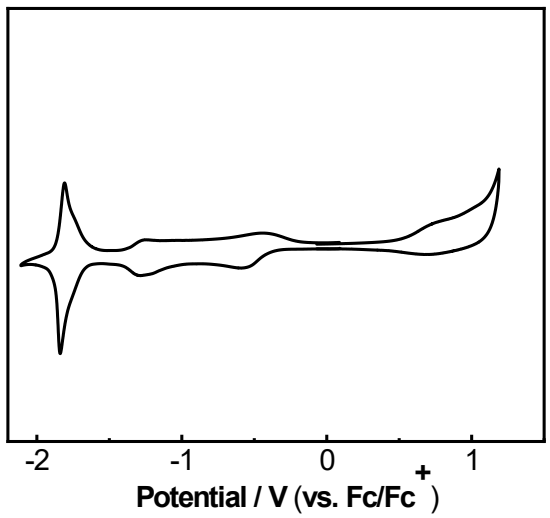

Figure S2. CV curve of PTBD

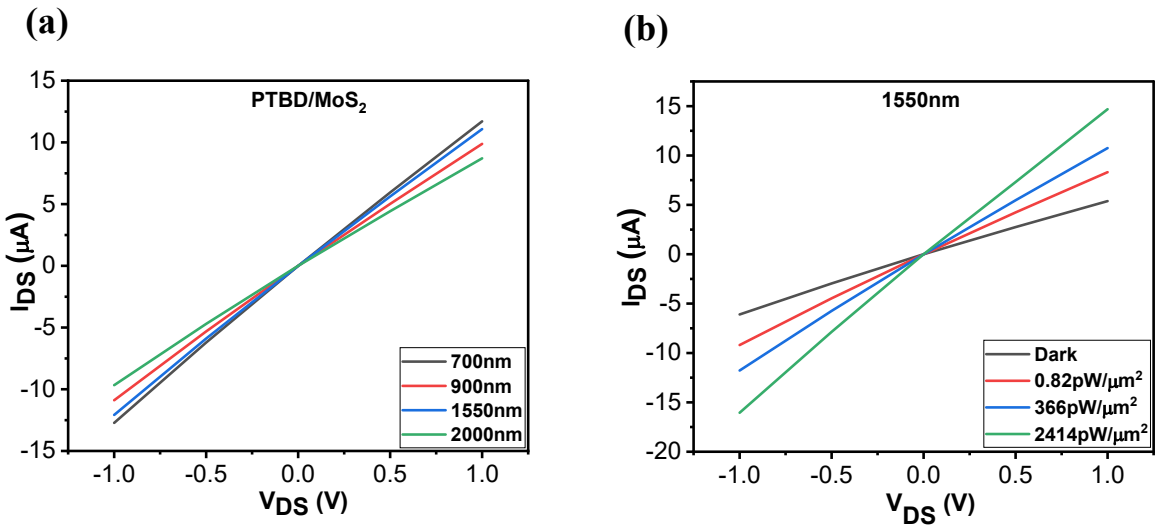

Figure S3. Output curve (I_{DS}-V_{DS}) (a) Wavelength-dependent measurements at 700 nm, 900 nm, 1550nm and 2000 nm. (b) Power-dependent measurements under dark and light with different power density at 1550 nm wavelength.

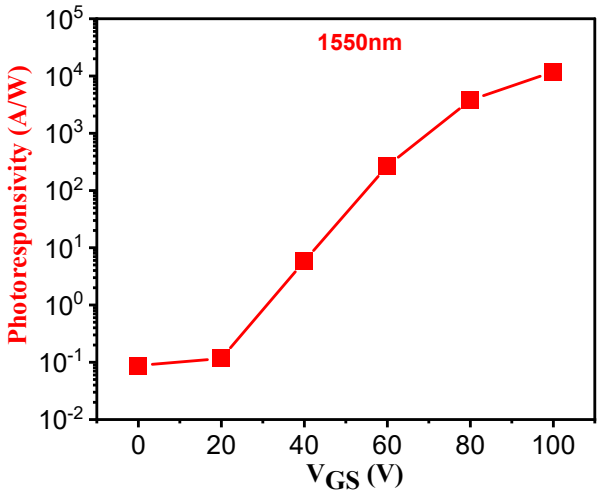

Figure S4. Gate-dependent maximum photoresponsivity at 19 pW/μm^2 power density.

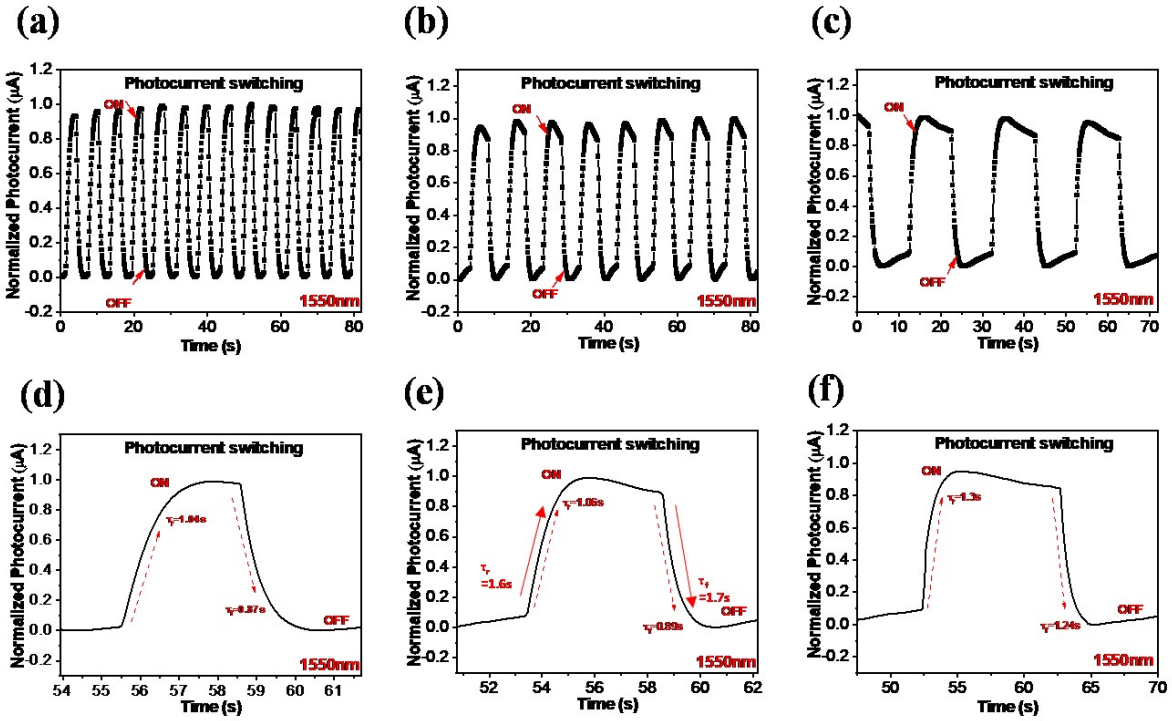

Figure S5. Photocurrent switching at different chopping (a,d) 3s, (b,e), 5s (c,f), 10s at 1550 nm wavelength.

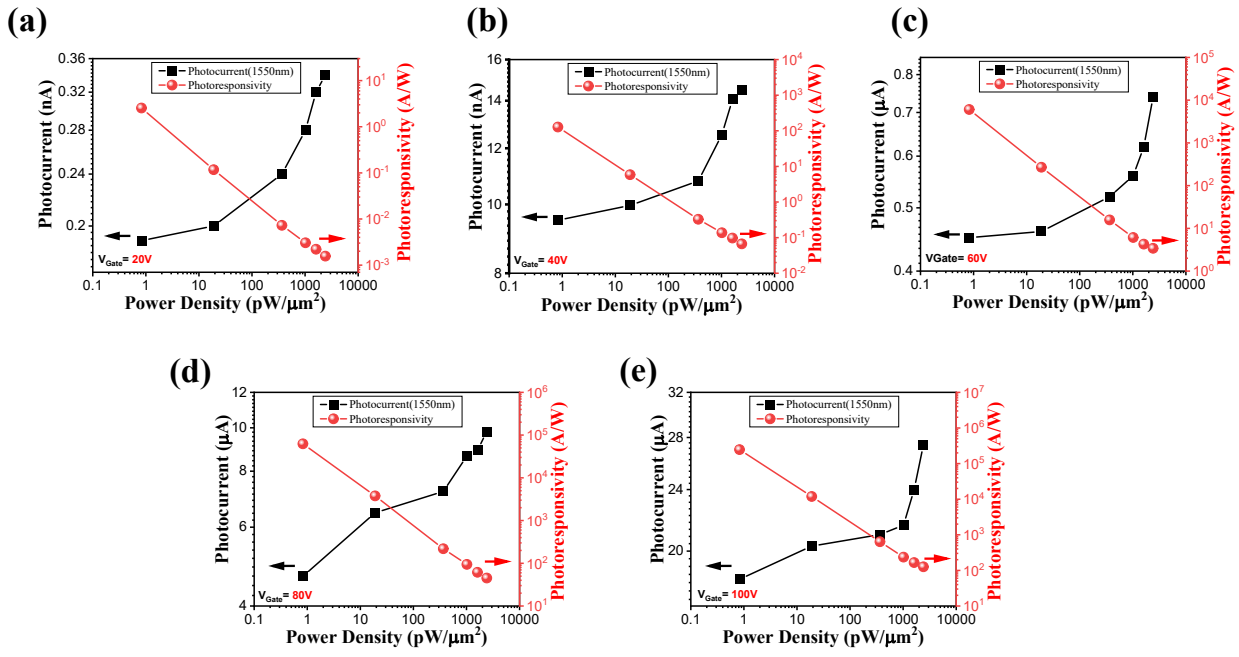

Figure S6. Power density dependent photocurrent and photoresponsivity for corresponding gate voltages (20 to 100 V) at wavelength 1550 nm (V_{Bias}=5 V).

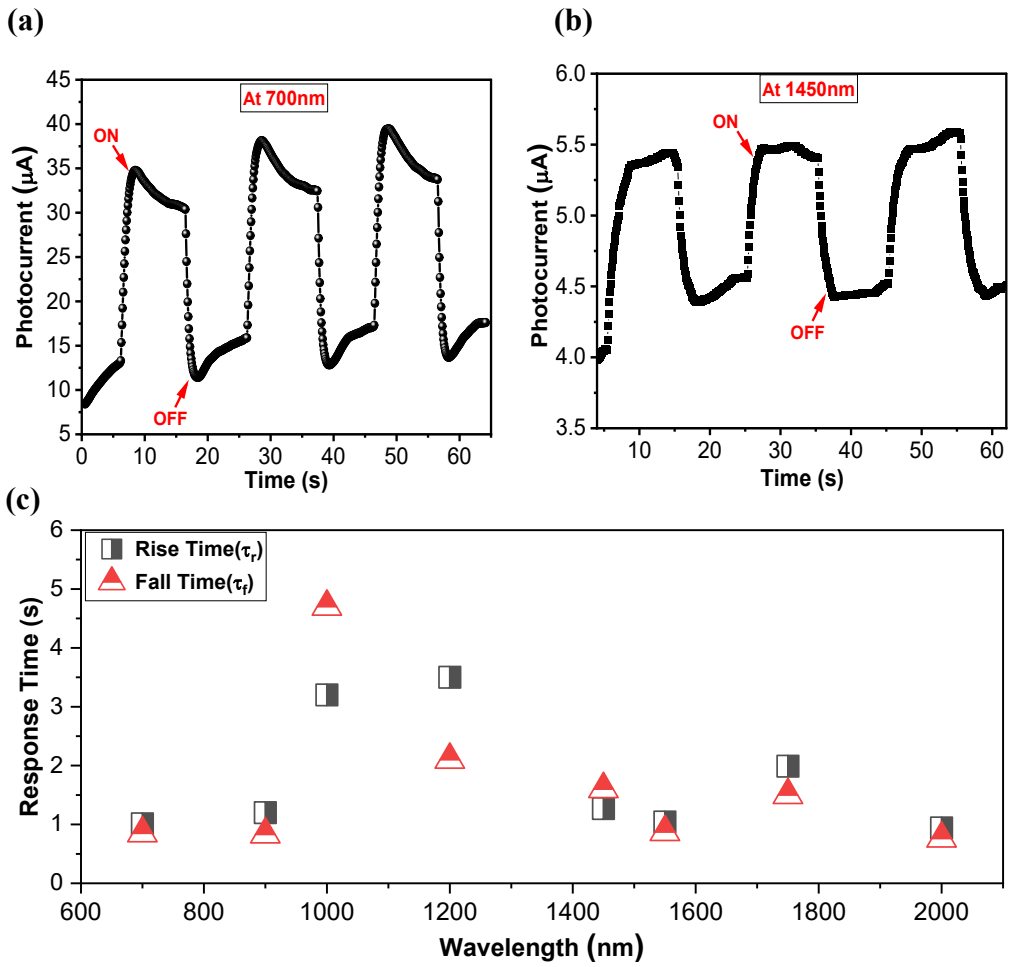

Figure S7. Photocurrent switching measurement of the PBTD/MoS_2 device at wavelength (a) 700 nm, (b) 1450 nm. (c) Response time for wavelength from 700 to 2000 nm (V_{Gate}=100 V and V_{Bias}=5 V).

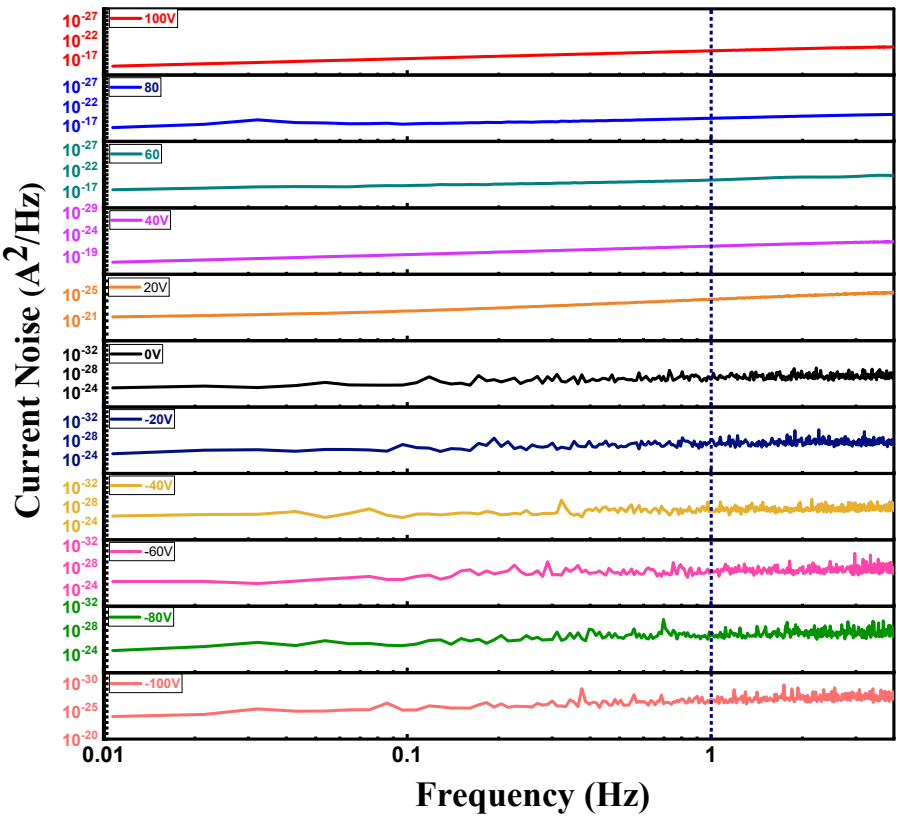

Figure S8. Frequency dependent current noise at different gate voltages (-100 to 100 V) and fix V_{Bias}= 5 V.

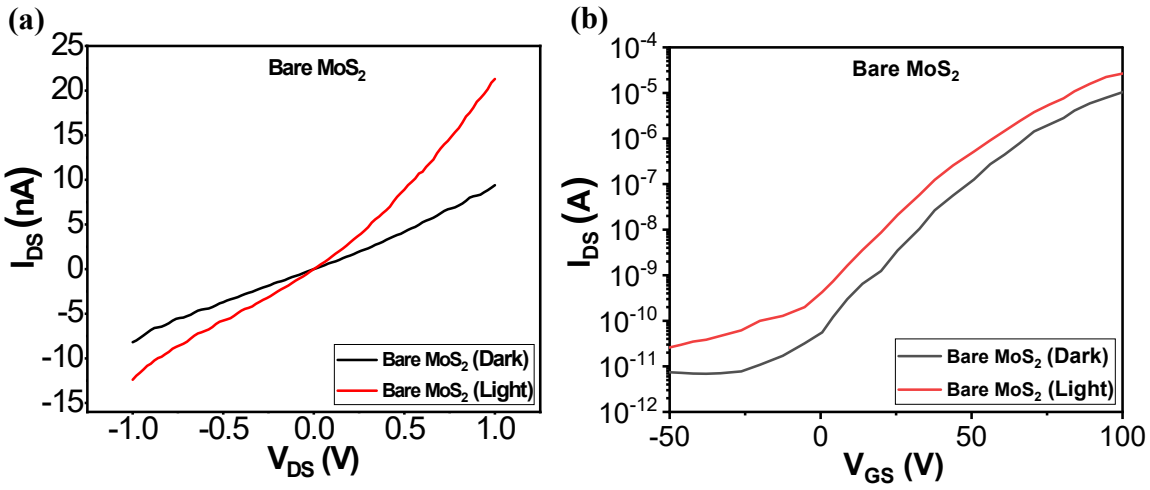

Figure S9. I_{DS}-V_{DS} and I_{DS}-V_{GS} curves of bare MoS_2 device with/without light illumination at 700 nm wavelength (power density= 4.94 pW/μm²).

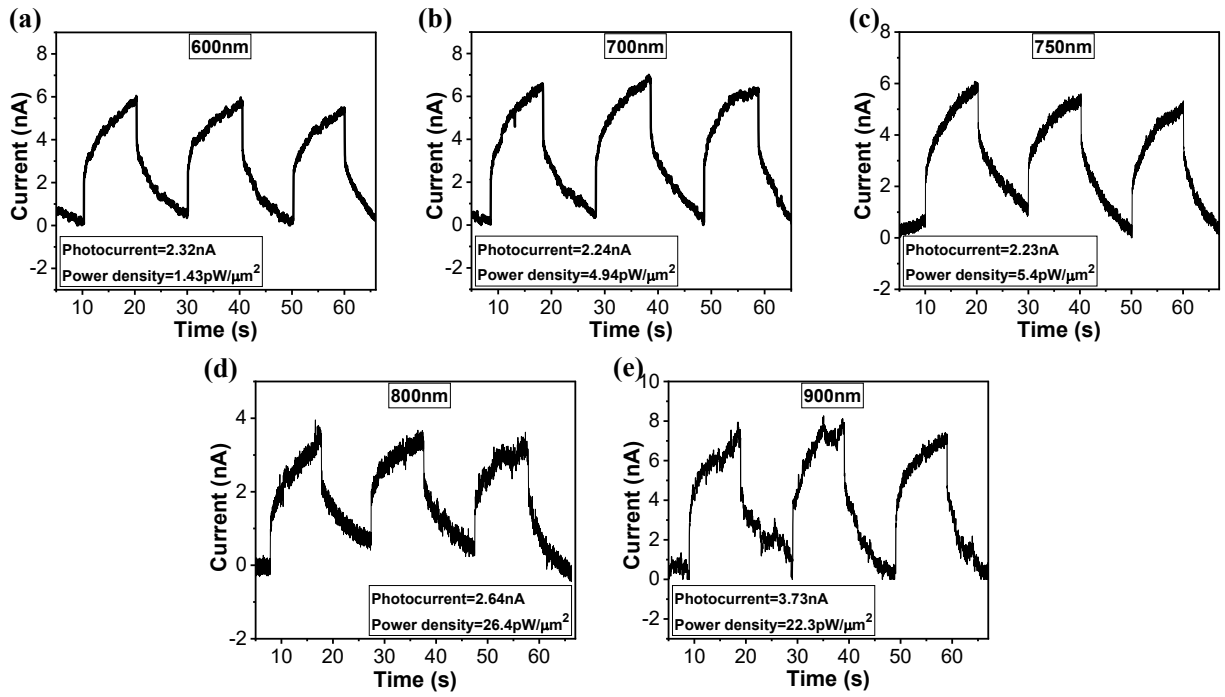

Figure S10. Photocurrent switching measurement of the bare MoS_2 device at wavelength (a) 600 nm (1.43 pW/μm²), (b) 700 nm (4.94 pW/μm²), (c) 750 nm (5.4 pW/μm²), (d) 800 nm (26.4 pW/μm²), (e) 900 nm (22.3 pW/μm²).

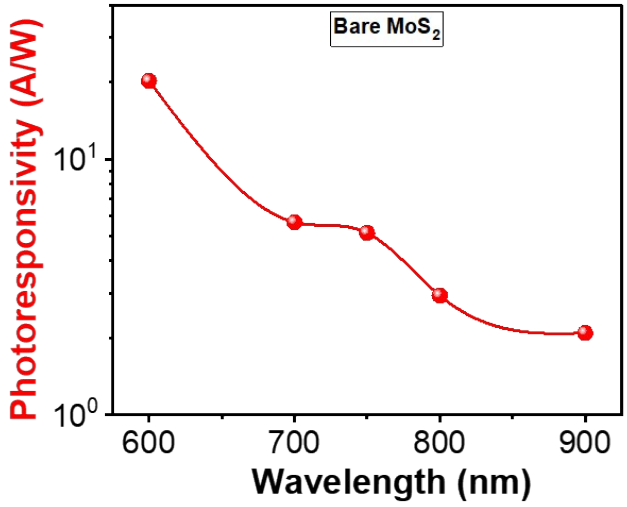

Figure S11. Photoresponsivity of bare MoS_2 and hybrid of PTBD/MoS_2.

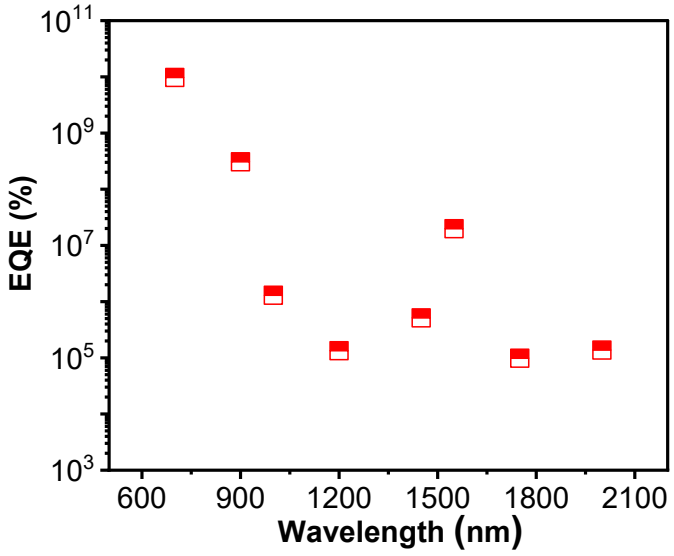

Figure S12. (a) Wavelength-dependent external quantum efficiency (EQE).

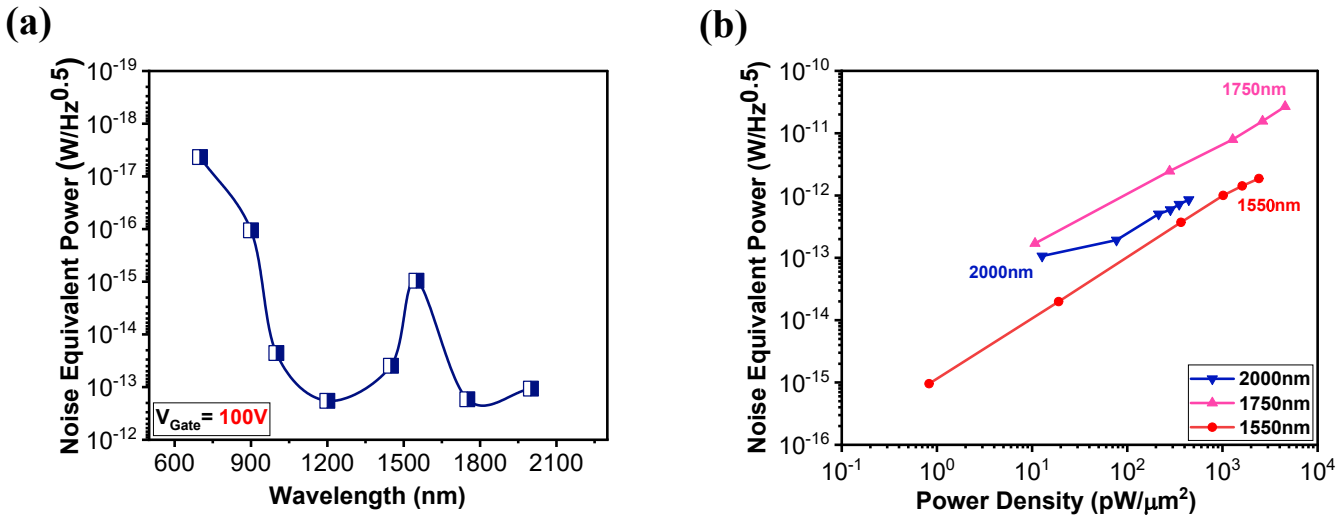

Figure S13. (a) Wavelength-dependent peak Noise Equivalent Power (NEP) at fix gate 100 V. (b) Power density dependent NEP for different wavelengths.

Table S1. Noise spectral density calculations at various gate voltages.

Gate Voltage (V)	Sampling rate Fs (Hz)	No. of Data Points (N)	Noise spectral density S_N (A/Hz$^{0.5}$) At f=1 Hz

-100	10.75	1000	2.548E-14
-80	10.742		2.938E-14
-60	10.740		2.887E-14
-40	10.741		2.720E-14
-20	10.739		8.621E-15
0	10.738		3.706E-14
20	10.743		7.850E-13
40	10.740		2.049E-11
60	10.742		1.360E-11
80	10.739		4.919E-10
100	10.743		2.363E-10

Table S2. Gate dependent detailed calculations of photoresponsivity, S_N, NEP and Detectivity at 1550nm and 2000nm wavelength.

1550nm					
Gate Voltage (V)	**Photocurrent (A)**	**Photoresponsivity (A/W)**	**S_N ($A/Hz^{0.5}$)**	**NEP ($W/Hz^{0.5}$)**	**Detectivity (Jones)**
40	9.5E-9	127.48	2.05E-11	1.07E-13	8.89E9
60	4.5E-7	6038.46	1.36E-11	2.25E-15	4.21E11
80	4.66E-6	62531.62	4.92E-10	3.78E-15	2.51E11
100	1.84E-5	246905.98	2.36E-10	9.57E-16	9.91E11

2000nm					
Gate Voltage (V)	**Photocurrent (A)**	**Photoresponsivity (A/W)**	**S_N ($A/Hz^{0.5}$)**	**NEP ($W/Hz^{0.5}$)**	**Detectivity (Jones)**

40	1.06E-9	0.92	2.05E-11	1.47E-11	6.45E7
60	1.17E-8	10.21	1.36E-11	1.33E-12	7.12E8
80	1.9E-7	165.72	4.92E-10	1.43E-12	6.65E8
100	2.53E-6	2206.72	2.36E-10	1.07E-13	8.86E9

Table S3. Wavelength dependent calculations of Maximum responsivity, NEP and Detectivity at fix gate 100 V.

Wavelength (nm)	**Responsivity (A/W)**	**Gate Voltage (V)**	**S_N ($A/Hz^{0.5}$)**	**NEP ($W/Hz^{0.5}$)**	**Detectivity (Jones)**
700	5.50E7	100	2.36E-10	4.30E-18	2.21E14
900	2234169.22			1.06E-16	8.97E12
1000	10466.67			2.26E-14	4.20E10
1200	1292.60			1.83E-13	5.19E9
1450	6006.32			3.93E-14	2.41E10
1550	246905.98			9.57E-16	9.91E11
1750	1387.27			1.70E-13	5.57E9
2000	2206.72			1.07E-13	8.86E9

Table S4. Comparison of our heterostructure with other reported organic and MoS_2 heterostructure

Type	Device structure	Spectral Range (nm)	R_{max} (A/W)	D_{max}* (Jones)	Ref.
Organic	PBTB polymer	400 - 2000	9.60×10^{-1}	$\sim 10^{10}$	57
	$TTD(DTC\text{-}2FIC)_2$	400 – 1400 (1200)	0.07 ($\pm$0.008)	$\sim 10^{11}$	58
	CO1-4Cl	400 – 1100(>900)	0.5	10^{12}	59
	CDT-TQ: $PC_{71}BM$	600 - 1400	0.11	2.40×10^{10}	60
	TQ: $PC_{71}BM$	400 - 1500	0.20	2×10^{11}	61
	PTB7-Th: PCBM	300 - 1000	0.01	4.6×10^{9}	62
	PMDPP3T:$PC_{61}BM$	350 - 1000	0.57	3.20×10^{11}	63
	TBzIC	350 - 1250	3.70×10^{-1}	2.24×10^{13}	64
MoS_2 Heterostructure	MoS_2/h-BN/G	1.4-3.1	180	2.6×10^{13}	65
	$MoS_2/G/WSe_2$	400-2400	1×10^{4}	1×10^{15}	66
	MoS_2/PbS nanoplates	800	4.5×10^{4}	3×10^{13}	67
	MoS_2/Si	400-1000	0.91	1.89×10^{13}	68
	MoS_2/GaAs	325-635	0.42	1.9×10^{14}	69
	PPh_3/MoS_2	520-850	3.92×10^{5}	2.36×10^{10}	70
	PbS Quantum dots/MoS_2	800-1100	10^{6}	10^{11}	71
	PTBD/MoS_2	700-2000	5.5×10^{7}	2.21×10^{14}	***This Work***

Synthesis of PTBD

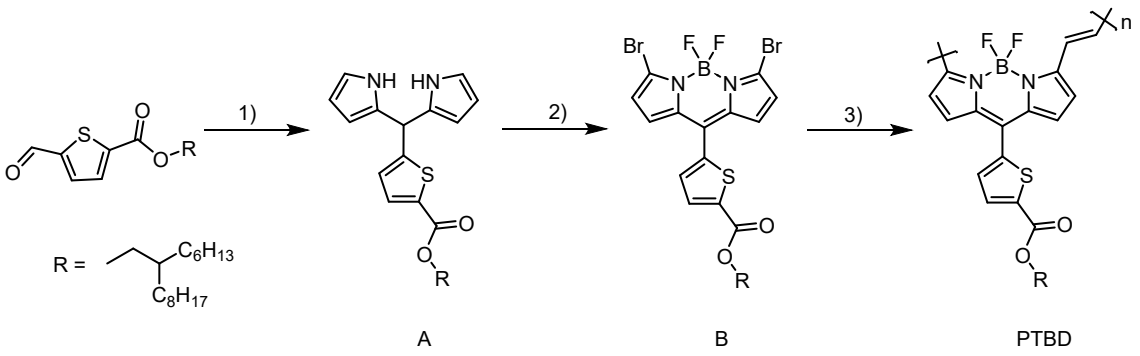

Figure S 14. Synthetic route to PTBD.

Procedure 1: An aldehyde-substituted thiophene (2.39 g, 6.28 mmol) was dissolved in pyrrole (21.1 g, 315.0 mmol). Argon is pumped into the mixture through a long needle for 30 minutes to remove oxygen. After that, $InCl_3$ (139 mg, 0.628 mmol) was added into the flask and the mixture was stirred at room temperature for 6 h. The reaction mixture was extracted by ethyl acetate and water for three times and washed twice with brine. The separated organic layer was dried over anhydrous Na_2SO_4 and concentrated under reduced pressure. The residue was purified by silica gel chromatography (petroleum ether: ethyl acetate=7:1) to afford compound A (2.51 g, yield:80%) as a pale-yellow solid. ^{1}H NMR (500 MHz, Benzene-*d6*) δ 7.72 (d, J = 3.8 Hz, 1H), 6.93 (s, 2H), 6.51 (dd, J = 3.8, 0.7 Hz, 1H), 6.23 (q, J = 2.6 Hz, 2H), 6.18 (q, J = 2.8 Hz, 2H), 6.01 (q, J = 2.8 Hz, 2H), 5.17 (s, 1H), 4.25 (d, J = 5.7 Hz, 2H), 1.68 (m, 1H), 1.36 – 1.24 (m, 24H), 0.94 – 0.87 (m, 6H).

Procedure 2: Compound A (2.51 g, 5.05 mmol) was dissolved in anhydrous THF (100 mL) and cooled to -78 °C under argon. When the temperature was constant, N-Bromosuccinimide (1.89 g, 10.62 mmol) was added in portions over 30 min. The mixture was stirred at -78 °C for 3 h. DDQ (1.16 g, 5.11 mmol) was added at same temperature. Then the reaction temperature slowly raised to room temperature and the solvent was evaporated on rotary evaporator under vacuum. Then the crude compound was dissolved in anhydrous DCM (100 mL). triethylamine (50.9 mmol, 7.03 mL) and $BF_3{\cdot}Et_2O$ (101.1 mmol, 13.50 mL) were added into the flask at room temperature for additional 12 h. The reaction mixture was extracted by dichloromethane and water and washed with brine. The separated organic layer was dried over anhydrous Na_2SO_4 and concentrated under reduced pressure. The crude product was purified by silica gel chromatography (petroleum ether: ethyl acetate=10:1) to afford Compound B (1.20 g, yield:34%) as orange red oil. ^{1}H NMR 400 MHz, Chloroform-*d*) δ 7.86 (d, J = 3.9 Hz, 1H), 7.42 (d, J = 3.9 Hz, 1H), 7.10 (d, J = 4.4 Hz, 2H), 6.59 (d, J = 4.4 Hz, 2H), 4.26 (d, J = 5.7 Hz, 2H), 1.81 – 1.72 (m, 1H), 1.32 (m, 24H), 0.87 (m, 6H).

Procedure 3: Compound B 63.7 mg (1 equiv), trans-1,2-bis(tri-n-butylstannyl) ethylene 55.6 mg (1 equiv), $Pd_2(dba)_3$ 1.7 mg (0.02 equiv) and P(*o*-Tol)$_3$ 4.4 mg (0.16 equiv) were added in a microwave vial. After adding 1 mL of dry toluene, the tube was sealed with a cap in a glovebox. The reaction vessel was placed in a CEM microwave reactor and heated to 120 °C using microwave irradiation (200 W) for 1 h. After cooling, the solvent was dispersed in methanol and then the precipitate was collected. The crude polymer was purified by Soxhlet extraction using acetone hexane and chloroform. The chloroform fraction was concentrated and poured into methanol. The precipitate was collected and dried in vacuo to afford polymer PTBD-2 (51.8 mg, yield:99%) as a black solid. ^{1}H NMR (400 MHz, Tetrachloroethane-*d2*) δ 7.97 – 7.82 (br, 1H), 7.11 – 7.65 (br, 1H), 7.37– 7.22 (br, 1H), 7.21 – 6.95 (br, 3H),

4.33 – 3.97 (br, 2H), 1.80 – 1.60 (br, 1H), 1.32 – 1.15 (br, 24H), 0.89 – 0.69 (br, 6H). GPC (TCB, polystyrene standard, 150 ^{o}C): Mn = 9.6 kDa, PDI = 2.6.